American Mineralogist, Volume 87, pages 433–444, 2002

Andalusite-sillimanite replacement (Mazarrón, SE Spain): A microstructural and TEM study

BERNARDO CESARE,[1,*] MARIA TERESA GÓMEZ-PUGNAIRE,[2] ANTONIO SÁNCHEZ-NAVAS,[2] AND BERNARD GROBETY[3]

[1]Dipartimento di Mineralogia e Petrologia, Università di Padova, Corso Garibaldi, 37, 35137 Padova, Italy
[2]Departamento de Mineralogía y Petrología, Facultad de Ciencias, Universidad de Granada. Fuentenueva s/n, 18002 Granada, Spain
[3]Institut de Mineralogie et Petrographie, Université de Fribourg, CH-1700, Fribourg, Switzerland

ABSTRACT

At Mazarrón, SE Spain, dacitic lavas of the Neogene Volcanic Province contain numerous xenocrysts and xenoliths with abundant andalusite that displays variable degrees of transformation to both fibrolite and coarse sillimanite. At the onset of replacement, andalusite dissolves along grain boundaries and (110) cleavage planes, probably assisted by fluids or melts. At the same time, fibrolite crystallizes together with plagioclase, cordierite, and graphite in newly formed embayments or in the adjacent matrix. With increasing reaction progress, fibrolite needles coalesce into coarser sillimanite prisms, and direct topotactic replacement of andalusite is observed.

The mutual crystallographic orientation of andalusite and sillimanite obtained from TEM investigation deviates slightly from the topotactic relationship proposed in the literature ($c_{And} \parallel c_{Sil}$, $a_{And} \parallel b_{Sil}$, $b_{And} \parallel a_{Sil}$). The two lattices are rotated by ~2.5° around a_{And} (= b_{Sil}). With this misorientation, the structurally equivalent $\{032\}_{And}$ and $\{302\}_{Sil}$ planes, which exhibit the smallest misfit between the two lattices, become parallel. Macroscopic interfaces with such orientations are rare. Microscopically, however, decomposition of faces into $\{032\}_{And} \parallel \{302\}_{Sil}$ and {110} facets are common. The mutual crystallographic orientation of the reactant and the product phases is, therefore, controlled by lattice misfit minimization. The prismatic shape of the final coarse sillimanite crystals, however, is controlled by kinetic factors. The reaction seems to proceed fastest parallel to the octahedral Al chains resulting in the development of crystals elongated along the *c* axis. The high activation energy and the large overstepping of the equilibrium temperature required for the transformation are probably responsible for the large differences in reaction progress observed in the samples from Mazarrón.

INTRODUCTION

Small entropy difference between the reactant and the product phase explains the large overstepping of the equilibrium temperature observed for polymorphic phase transformations and the metastable persistence of the low-temperature polymorph within the stability field of the high-temperature one (e.g., Walther and Wood 1984). Transformations involving Al-silicate polymorphs constitute natural examples of reactions for which a large overstepping of the equilibrium boundary is to be expected. Sillimanite-producing reactions exhibit an additional complexity in the appearance of two distinct morphologies: fibrous ("fibrolite") and coarse-grained sillimanite. The sluggish reaction rates and the poorly known factors that control sillimanite size and shape are probably the main reasons why a wealth of reaction microstructures are found in natural samples, and why the location in *P-T* space of the And-Sil equilibrium is still debated. Although there is a general consensus toward the experimental determinations of Holdaway (1971), alternative phase boundaries at higher temperature have been proposed (discussion in Pattison 1992).

In nature, andalusite together with fibrolite or coarse-grained sillimanite are commonly observed over a large distance beyond the first appearance of the high-temperature polymorph, corresponding to a large range of inferred temperatures. This is particularly evident in contact aureoles, characterized by fast heating rates and by the short duration of the metamorphic event. For example, in the Mt. Raleigh pendant (British Columbia), the assemblage andalusite-sillimanite can be observed over 3 km from the first appearance of fibrolite toward the contact. This distance corresponds to a maximum estimated overstepping of the equilibrium boundary of ~60 °C (Kerrick and Woodsworth 1989).

Two reaction mechanisms for the andalusite-sillimanite transformation can be distinguished: a crystallographically controlled, solid-state reaction (Harker 1939; Rosenfeld 1969; Vernon 1987; Kerrick and Speer 1988; Kerrick and Woodsworth 1989) and an indirect process of dissolution-crystallization, commonly involving a fluid phase and other minerals (e.g., Glen 1979). Based on optical observations, Vernon (1987) proposed the following crystallographic relationships for the solid-

* E-mail: bernardo.cesare@unipd.it

state transformation between the two polymorphs: $c_{And} \parallel c_{Sil}$, $a_{And} \parallel b_{Sil}$, $b_{And} \parallel a_{Sil}$ (mineral abbreviations after Kretz 1983). Because of the similarity in molar volumes of these phases (ΔV of approximately 2%), this topotactic replacement can be considered a "volume-for-volume" reaction. For the dissolution/precipitation replacement And = Sil, Glen (1979) suggested the same "subdomain" mechanism previously proposed for the Ky = Sil reaction (Carmichael 1969). The dissolution and the precipitation steps occur at distinct locations ("subdomains") and involve phases other than the Al silicates (e.g., micas). If the system is closed on a scale that includes a complete set of subdomains, the appearance and disappearance of these non-Al-silicate phases balance each other, so that the net reaction over all subdomains corresponds to the polymorphic transformation And = Sil.

Andalusite xenocrysts and andalusite-bearing xenoliths found in the dacitic lavas of Mazarrón, SE Spain, exhibit different replacement microstructures and show various degrees of transformation progress to sillimanite/fibrolite. Optical and transmission electron microscopy (TEM) of reaction microstructures allows the progress of the And = Sil reaction to be examined as a function of time. The TEM analysis of the crystallographically controlled solid-state replacement microstructures reveals a small but systematic deviation from the lattice orientation relationships given in the literature. This deviation is explained using lattice misfit minimization arguments.

GEOLOGIC BACKGROUND

The andalusite-sillimanite reaction microstructures have been studied in xenoliths and xenocrysts enclosed in the Miocene lavas of Mazarrón, which are part of the Neogene Volcanic Province of SE Spain (e.g., Benito et al. 1999; Turner et al. 1999). Volcanic rocks are mostly represented by cordierite-bearing dacites of high-K, calc-alkaline affinity, erupted at about 9 Ma (Bellon et al. 1983) as the consequence of the opening of the Alborán Sea. The dacites and the enclosed crustal xenoliths were described by Molin (1980): they have many similarities to the rocks of the neighboring volcanic edifice of El Joyazo with which they are considered to share a crustal anatectic origin (Cesare and Gómez-Pugnaire 2001, and references therein).

The fresh dacite contains millimeter-sized phenocrysts of plagioclase, biotite, pyroxene, amphibole, and cordierite in an abundant glassy matrix. Xenocrysts of foreign provenance include garnet, cordierite with euhedral overgrowths of magmatic origin, sillimanite, spinel, and andalusite. Andalusite occurs in pink subhedral crystals up to 2 cm across and 7 cm in length (Fig. 1), some with abundant graphite inclusions as in the chiastolite variety. Macroscopically, the centimeter-sized andalusite can be observed to contain variable amounts of sillimanite. Some xenocrysts consist entirely of sillimanite (Fig. 2) that preserves the shape and arrangement of graphite inclusions diagnostic of former chiastolite. A reaction rim consisting of cordierite, hercynitic spinel, and plagioclase commonly occurs at the contact between dacite and Al_2SiO_5 xenocrysts. The presence of this rim supports the contention that, unlike in the example from the Macusani volcanics, Peru (Pichavant et al. 1988), andalusite and sillimanite are not magmatic in origin.

The dacite also typically contains abundant crustal xenoliths. Compared to the well-known examples of El Joyazo (e.g., Zeck 1970), crustal xenoliths at Mazarrón have a wider range of mineral compositions, and contain a higher abundance of cordierite and andalusite as well as minor amounts of garnet. The presence of glass in the xenoliths, both as interstitial pockets and as primary melt inclusions trapped in most minerals, the absence of quartz and K-feldspar, and the Al_2O_3-rich (23–33 wt%), SiO_2-poor (45–50 wt%) bulk composition (Benito et al. 1999), support the model originally proposed at El Joyazo by Zeck (1970) that the xenoliths represent restites. These restites derived from anatexis of pelitic protoliths and extraction of large amounts of anatectic melts, preserved in the melt inclusions (Cesare and Gómez-Pugnaire 2001). Microstructural analysis has demonstrated that partial melting in the xenoliths was accompanied by development of a marked foliation. This has been interpreted as evidence that melting took place when the metapelitic protolith was still a coherent body, i.e., before enclosure of the xenoliths in the host dacite (Cesare and Gómez-Pugnaire 2001). Because the xenoliths contain porphyroblasts of andalusite with similar size, type, and arrangement of inclusions as observed in the xenocrysts, we infer that andalusite xenocrysts formed by fragmentation of the xenoliths either at the time of, or after enclosure by the host dacite.

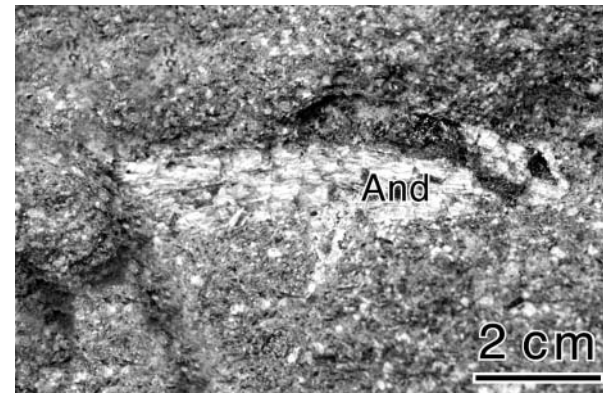

FIGURE 1. Andalusite xenocryst (And) enclosed in dacitic lava from Mazarrón.

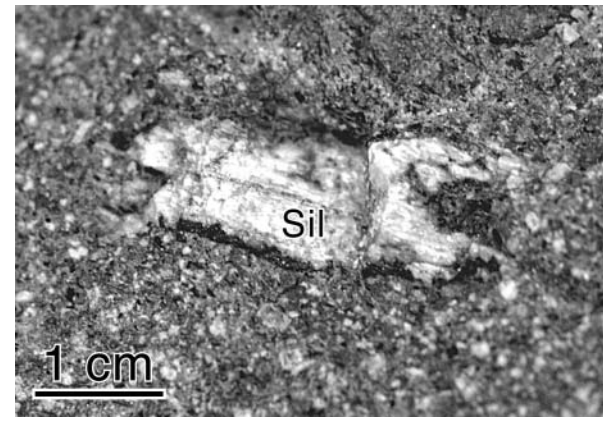

FIGURE 2. Sillimanite xenocryst (Sil), pseudomorph after andalusite.

The *P-T* conditions of equilibration of the xenoliths and xenocrysts are not well constrained. By comparison with the dacite of El Joyazo (Cesare et al. 1997; Cesare and Gómez-Pugnaire 2001), we may infer that the mineralogical assemblage of the xenoliths indicates temperatures >800 °C, and that the lava was around 900 °C, whereas pressure must have been <4 kbar (Holdaway 1971) to account for the stability of andalusite before enclosure in the lava (e.g., Soto and Platt 1999). As discussed for the xenoliths of El Joyazo, the persistence of biotite in the xenoliths at temperatures up to 900 °C is not surprising, if the absence of quartz in the xenoliths and the high TiO_2 contents of biotite are considered (Cesare et al. 1997).

PETROGRAPHY

Samples of both coarse-grained xenoliths and single xenocrysts have been selected for microstructural analysis and subsequent TEM characterization. These samples show variable degrees of andalusite replacement by sillimanite, ranging from very little to virtually complete.

Sillimanite is present in all samples. It displays different microstructures as well as variable grain size and crystallographic orientations relative to the primary andalusite. In the following microstructural descriptions, we have adopted the distinction between fibrolite and sillimanite proposed by Pattison (1992): the fine grained (<2 μm), needle-like variety of sillimanite is called fibrolite (Fbr), whereas the term sillimanite refers to the coarse-grained variety, generally with a prismatic habit.

Microstructures in xenoliths

Andalusite-bearing xenoliths range in size from 1 to ~20 cm, and include fine-grained gneisses, coarse-grained graphitic schists, and hornfelses. Hornfelses contain plagioclase, cordierite, andalusite, fibrolite, sillimanite, and graphite with minor amounts of biotite, garnet, hercynite, ilmenite, and corundum. Biotite is generally scarce (<5%), and occurs as rounded inclusions in cordierite and andalusite. Quartz, K-feldspar, and mullite have not been observed. The occurrence of primary melt inclusions indicates that the host minerals (including andalusite) have grown within the xenoliths in the presence of a melt phase. This phenomenon cannot be attributed to crystallization from a melt, as could be expected in the single phenocrysts of the lava, and must be related to an event of partial melting [see discussion in Cesare et al. (1997) and Cesare and Maineri (1999)]. The xenoliths often show a well-developed foliation, that wraps around porphyroblasts of plagioclase and andalusite that contain melt inclusions. This indicates that the foliation is syn-anatectic (Cesare and Gómez-Pugnaire 2001).

Pelitic xenoliths contain abundant fibrolite, which occurs mainly in the rock matrix anastomosing around andalusite porphyroblasts. The boundaries of andalusite commonly show embayments (Fig. 3) filled by a mixture of plagioclase (An_{60}), randomly oriented fibrolite, and local cordierite (X_{Mg} = 0.46). Fibrolite can also be associated with very fine-grained graphite, either in thick segregations defining the foliation, or together with other silicates (e.g., plagioclase) in a network of veinlets replacing andalusite along embayments (Fig. 4). In the above microstructures, fibrolite is randomly oriented, without a relationship to the crystallographic orientation of the adjacent andalusite. Although it is seldom in direct contact with andalusite, one exception is where fibrolite, associated with graphite, seems to be located preferentially along (110) planes of andalusite (Fig. 5). However, this microstructure is controversial. It could be interpreted as evidence of either replacement of andalusite by oriented fibrolite or, conversely, as growth of chiastolite-like andalusite enclosing fibrolite. The transition of fibrolite to sillimanite is observed as the coalescence and coarsening of several parallel needles to produce discrete prisms with cross sections >100 μm (Fig. 6; see also "bladed" sillimanite of Vernon 1987). The sillimanite formed by coarsening of favorably oriented fibrolite forms either crystallographically oriented prisms in andalusite, or randomly distributed crystals, both inside andalusite and in the rock matrix.

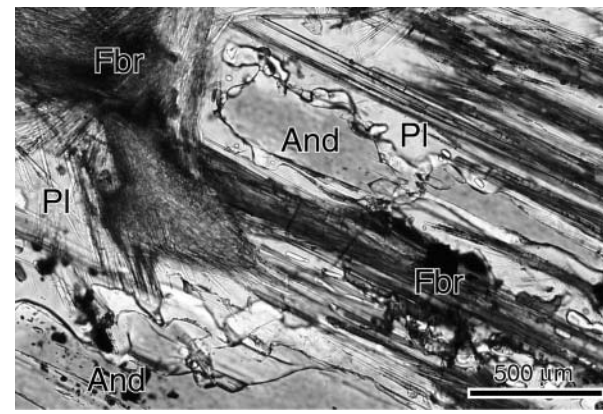

FIGURE 3. Photomicrograph depicting microstructural relationships between andalusite and fibrolite (Fbr). Andalusite displays a resorbed appearance with embayed grain boundaries and is surrounded by fibrolite, plagioclase (Pl) and/or cordierite. Fibrolite is not in contact with andalusite. Crossed polarizers.

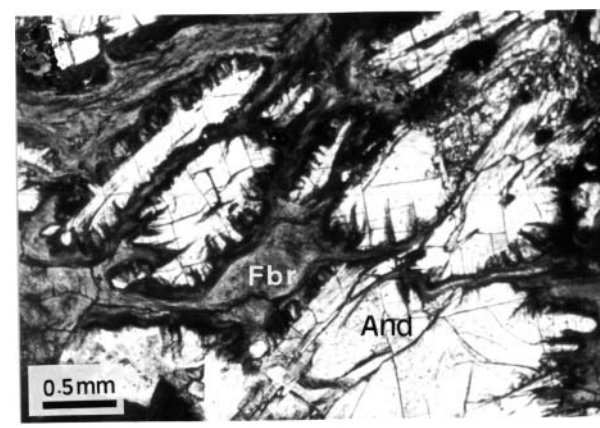

FIGURE 4. Advanced replacement of andalusite by fibrolite. Fibrolite strands surround lobate relics of a single, optically continuous andalusite porphyroblast. Crossed polarizers.

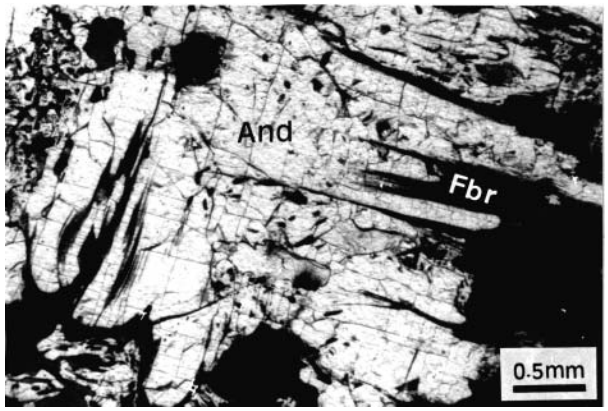

FIGURE 5. Fibrolite arranged at right angles to and apparently following the (110) traces of an andalusite porphyroblast. Fibrolite is associated with fine-grained graphite. Plane-polarized light.

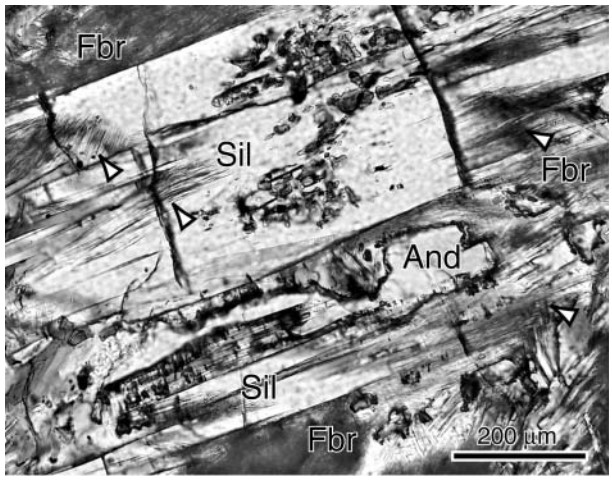

FIGURE 6. Prismatic sillimanite (Sil) with terminations merging into fibrolite aggregates. Arrows indicate areas where the *c* axes of intergrown Sil and Fbr are misoriented. Crossed polarizers.

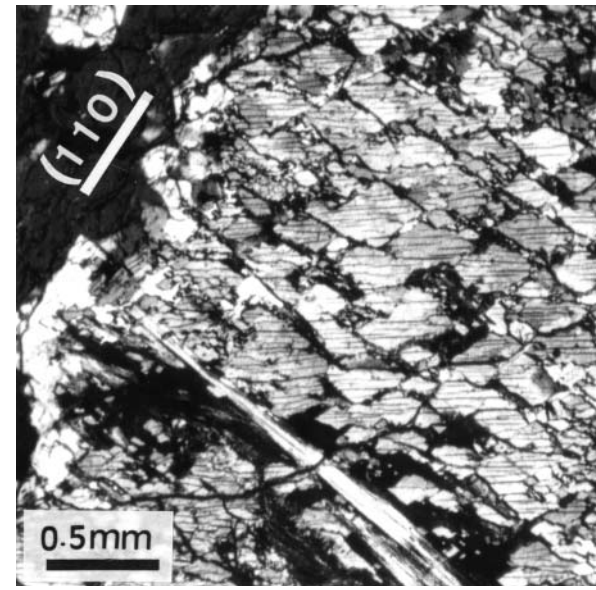

FIGURE 7. Complete replacement of andalusite by coarse sillimanite, preserving the traces of the prismatic faces of the primary andalusite crystal. Crossed polarizers.

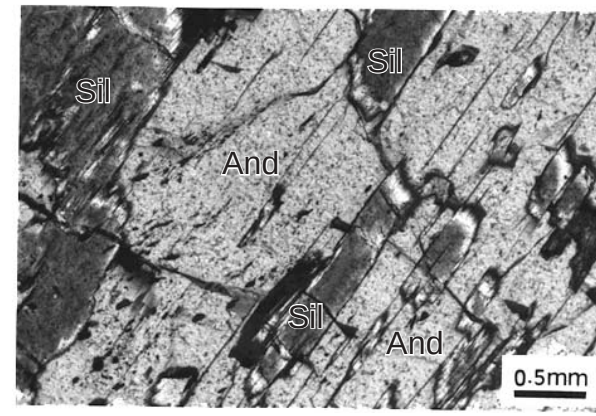

FIGURE 8. Small crystals of prismatic sillimanite (darker grey) within an andalusite porphyroblast. The *c* axes of andalusite and sillimanite are almost parallel to the section of the picture. Crossed polarizers.

Microstructures in xenocrysts

The differences between the replacement microstructures observed in single xenocrysts and those found in xenoliths are that: (1) fibrolite is less abundant; (2) the pseudomorphic replacement of andalusite, mostly by oriented sillimanite, may go to completion; (3) a symplectic reaction rim consisting of hercynite, plagioclase, and cordierite commonly develops between the xenocrysts and the host lava.

Three different orientation relationships were found between coarse sillimanite prisms and the remaining andalusite. Most sillimanite occurs as oriented prisms with their *c* axes approximately parallel to that of the remaining andalusite (Figs. 7 and 8). The second and third type consist of elongate crystals, either with *c* axes lying within in the {110} cleavage planes of former andalusite (Fig. 9) or with random orientation (Fig. 10).

The rare fibrolite occurring in the xenocrysts is, like in the xenoliths, commonly associated with silicates other than andalusite and forms aggregates that may coalesce into coarser sillimanite. Microstructural relationships indicate that fibrolite is generally overgrown by sillimanite with a defined crystallographic orientation relationship relative to the primary andalusite.

The crystallographic relationships between andalusite and oriented sillimanite are best appreciated in basal sections of the least-transformed andalusite xenocrysts, in which fibrolite and randomly oriented sillimanite are rare (Fig. 11). The orientation of sillimanite prisms in andalusite is such that the *c* axes of both phases are (almost) parallel, whereas the *a* and *b* axes are interchanged (Vernon 1987). An angular deviation of 5 to 10° between the *c* axes of adjacent crystals is often observed (also noted by Rosenfeld 1969). In many cases, the deviation follows a regular pattern with two main orientations of the sillimanite *c* axes at about ±2–3° from the andalusite *c* axis. Almost all prism faces with an overall orientation parallel to (100)

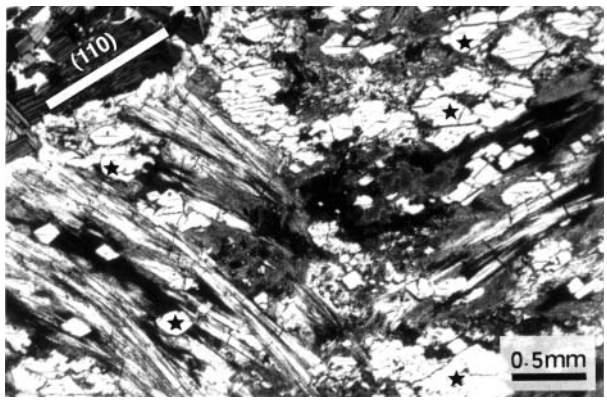

FIGURE 9. Complete pseudomorphic replacement of andalusite by sillimanite. Stars label prisms with *c* axes subparallel to the c axes of former andalusite, oriented normal to the plane of picture. Two other sets of crystallographically controlled sillimanite can be observed, with their c axes lying in the (110) planes (or equivalent) of andalusite. Crossed polarizers.

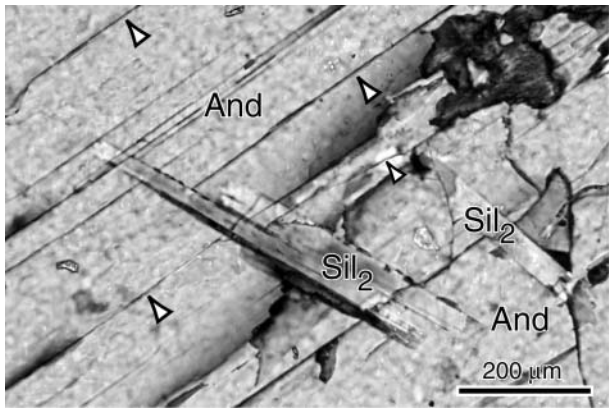

FIGURE 10. Prismatic, non-topotactic sillimanite (Sil_2) in andalusite. Arrows point to the traces of andalusite (110). The And-Sil_2 boundaries are sharp and clear, without other phases involved. Crossed polarizers.

or (010) are decomposed into {110} facets (Fig. 11b).

In summary, four types of "sillimanite" can be clearly distinguished. (1) Crystallographically controlled, coarse-grained sillimanite replacing andalusite (hereafter referred to as Sil_1, Fig. 11). (2) Randomly oriented coarse-grained sillimanite (Sil_2), preferentially intergrown with andalusite. Sil_2 may also develop along former andalusite cleavage planes (Fig. 9) or within the rock adjacent to andalusite. (3) Fibrolite occurring within enbayments of andalusite and along fractures within andalusite (Fig. 3): this is the main type of fibrolite. It is seldom in contact with andalusite and is commonly associated with plagioclase and/or cordierite. (4) Fibrolite, associated with graphite, either replacing andalusite along corroded grain boundaries or along andalusite cleavage planes (Fig. 5). The product of direct replacement of andalusite is commonly coarse-grained Sil_1. Except for some rare and difficult to interpret cases (Fig. 5), fibrolite is never found intersecting andalusite grain boundaries.

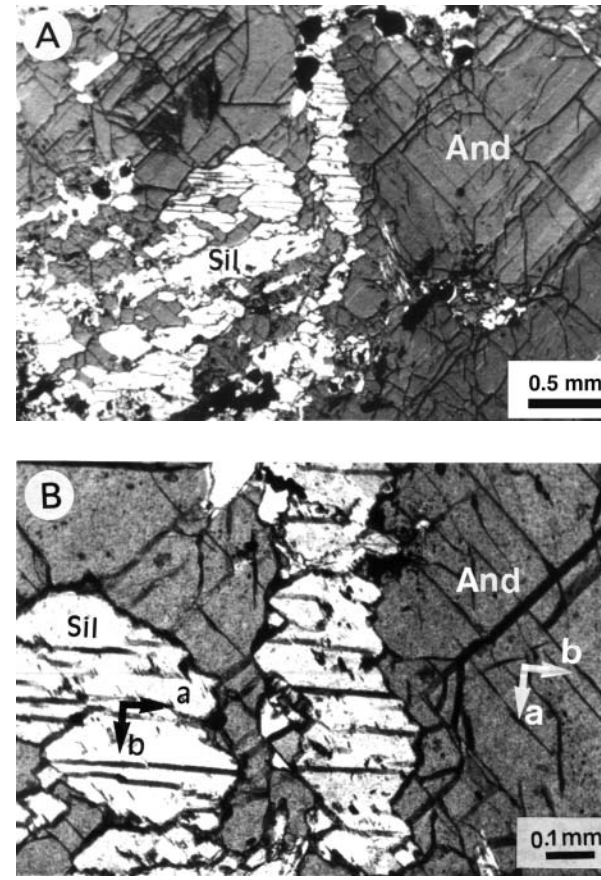

FIGURE 11. Crystallographic relationship between andalusite and crystallographically controlled Sil_1 (crossed polarizers). **(a)** Andalusite crystal partially replaced by prismatic sillimanite. The presence of the (110) cleavage planes of andalusite and (010) cleavages of sillimanite indicate that the thin section is cut close to the basal plane of both phases. **(b)** Detail of **a**, showing the relationships between the cleavages in Sil_1 and andalusite.

Evidence for direct transformation of andalusite to sillimanite

Because some of the microstructural relationships between andalusite and Sil_1 might be interpreted as indicating either simultaneous growth or replacement, and because these alternative hypotheses have a deep influence on the discussion of TEM results, it is crucial to provide strong evidence in support of either process.

The general obervation of resorbed andalusite boundaries (e.g., Fig. 6) indicates andalusite dissolution, but is not proof of replacement, as andalusite might have dissolved after simultaneous growth with sillimanite. More definitive evidence is provided by the microstructure of Figure 12, which shows a fractured crystal of andalusite, with the fracture filled with plagioclase and sillimanite. The oriented crystals of Sil_1 pass with continuity from andalusite to the fracture, and have an euhedral shape. This microstructure indicates that Sil_1 was growing, or continuing to grow, after crystallization of andalusite. Thus,

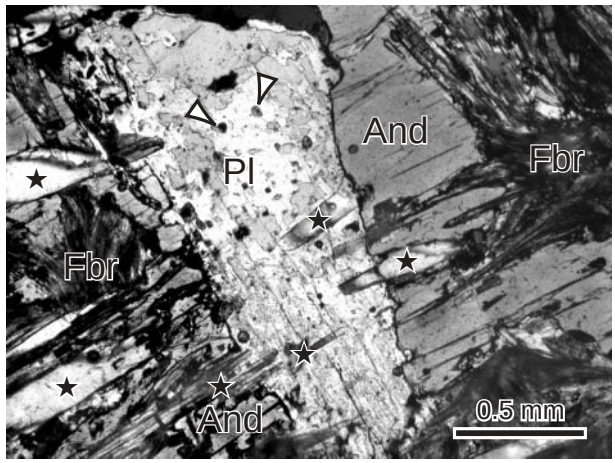

FIGURE 12. Microboudinaged porphyroblast of andalusite, with fracture filled with plagioclase. Some oriented crystals of Sil_1 (stars) pass with continuity from andalusite to plagioclase. Other sillimanite crystals occur in the plagioclase-filled fracture. Plagioclase contains primary glass inclusions (arrows). Crossed polarizers.

we conclude that in the studied xenoliths, Sil_1 replaced andalusite. Because there is a slight angular misorientation (~5°) between the two fragments of andalusite, and because sillimanite prisms show signs of weak bending, we also conclude that the replacement of andalusite by sillimanite was accompanied by deformation of the xenoliths. As discussed above, this syntectonic crystallization is likely to have occurred when the anatectic metapelites were still constituting a coherent body in which stress could be effectively transferred.

CHEMICAL DATA

Andalusite and sillimanite with varying microstructures from six samples were analyzed by wavelength dispersive methods using a CAMECA electron microprobe at the University of Granada, using synthetic standards. Accelerating voltage was 15 kV and sample current was 15 nA. Analytical precision was about ±1.5% relative for a concentration >1 wt%. Results are given in Table 1. Owing to its very fine grain-size, fibrolite could not be analyzed. Andalusite and both types of sillimanite are close to stoichiometric Al_2SiO_5. Fe_2O_3 is present in all polymorphs in similarly low amounts (<0.5 wt%, average ~0.25), and Mn_2O_3 is negligible. These data, and the equal Fe_2O_3 concentrations in polymorphs from the same thin section, indicate that phase relationships between andalusite and sillimanite were probably not affected by minor element partitioning.

TEM STUDY OF THE TOPOTACTIC ANDALUSITE-SILLIMANITE (SIL_1) REPLACEMENT

The TEM study was undertaken to characterize the mechanisms of direct replacement of andalusite by sillimanite, and to understand the slight, but systematic misorientation of the crystallographic axes between the two polymorphs.

Analytical procedures

Discs, 3 mm in diameter, were prepared from petrographic thin sections cut approximately parallel to the *c* crystallographic axes of the intergrown andalusite and sillimanite. The samples were further thinned using a Gatan 600 ion mill. Sillimanite is slower to mill than andalusite and isolated sillimanite prisms within andalusite show up as promontories along the thinned borders of the samples. The TEM observations of the carbon-coated samples were made using a PHILIPS CM-20 scanning transmission electron microscope (STEM) operated at 200 kV and equipped with a solid-state, ultrathin-window EDAX energy dispersive spectrometer (EDS). An objective aperture of 40 μm was used, thus limiting the reflections contributing to the lattice fringe contrast in HRTEM images to *d*-values >0.4 nm.

Results

Sillimanite crystals found in the andalusite host range from macroscopically visible prisms down to lamellae with dimensions well below the resolution of an optical microscope (Fig. 13a–c). The SAED patterns of all crystals revealed a slight misorientation of the *c* axes of both phases equivalent to a rotation by ≈2.5° around $a_{And} = b_{Sil}$, causing a change in the orientation of the lattice fringes at the boundary. Facetting of the interfaces on a microscopic level is common. In addition to facets with $\{110\}_{And}$ orientations already familiar from the thin section micrographs (Fig. 11b), a second set of facets with traces at approximately 53° from the $\{110\}_{And}$ lattice fringes is present (Fig. 14). The remaining lattice mismatch along the faceted boundaries is relieved by interface dislocations (Fig. 15).

The shape and orientation of the Sil_1 crystal is variable, most of the prisms are parallel to the *c* axis (Fig. 13) but some sillimanite lamellae are intermediate between the c_{And} axis and the $[011]_{And}$ direction (Fig. 14).

The mechanism of andalusite-sillimanite topotactic replacement

The structures of sillimanite and andalusite are very similar, particularly the almost identical arrangement of octahedral chains found in both minerals (e.g., Papike 1987). Both structures consist of straight chains of edge-sharing AlO_6 octahedra that extend along their *c* axes and are linked by other Al polyhedra and SiO_4 tetrahedra. In sillimanite, the Al polyhedra linking the octahedral chains are tetrahedra whereas in andalusite they are trigonal bipyramids (e.g., Putnis 1992). Despite this similarity, there are considerable differences in the lattice parameters of both phases. At room temperature, the mismatch is largest between b_{And} and a_{Sil} and smallest between a_{And} and b_{Sil}. These relationships do not significantly change with temperature (Winter and Ghose 1979). It is these lattice mismatches that exert the control on the sillimanite lattice orientation.

The slight misorientation of the sillimanite lattice relative to the andalusite host can be explained by analogy with results obtained from experiments on the topotactic transformation of andalusite to mullite, an aluminum silicate with a structure very similar to sillimanite (Hülsmans et al. 2000a). This transformation proceeds by a bulk mechanism and the fastest mullite reaction fronts are parallel to $(001)_{Mul}$ and advance along c_{And}.

TABLE 1. Representative electron microprobe analyses of andalusite and sillimanite in xenocrysts and xenoliths of Mazarrón

Sample	MA4	MA4	MA5	MA5	MA5-4	MA5-4	MA5-5	MA5-5	MA5-6	MA5-10
Phase	And	Sil_2	Sil_2	Sil_1	And	Sil_1	Sil_1	Sil_2	And	And
SiO_2	36.78	36.68	36.09	36.56	36.59	36.69	36.64	36.80	36.38	36.48
TiO_2	0.03	0.00	0.03	0.00	0.04	0.00	0.01	0.01	0.03	0.02
Al_2O_3	62.86	62.64	63.04	62.60	62.81	62.91	62.82	62.68	62.55	62.50
Fe_2O_3	0.17	0.17	0.21	0.25	0.22	0.22	0.21	0.28	0.37	0.20
Mn_2O_3	0.01	0.02	0.00	0.00	0.01	0.00	0.01	0.01	0.00	0.00
MgO	0.02	0.00	0.01	0.01	0.03	0.01	0.02	0.02	0.03	0.03
Na_2O	0.01	0.01	0.03	0.02	0.00	0.01	0.00	0.02	0.02	0.02
K_2O	0.00	0.01	0.02	0.00	0.01	0.00	0.00	0.02	0.00	0.01
Total	99.88	99.53	99.44	99.44	99.69	99.84	99.70	99.82	99.37	99.23
Formula proportions of cations based on 20 O atoms										
Si	3.978	3.981	3.924	3.973	3.966	3.970	3.970	3.984	3.960	3.971
Al	8.015	8.014	8.081	8.020	8.026	8.026	8.025	8.000	8.027	8.022
Ti	0.002	0.000	0.002	0.000	0.003	0.000	0.001	0.001	0.002	0.001
Fe^{3+}	0.014	0.013	0.018	0.020	0.018	0.018	0.017	0.023	0.030	0.016
Mn^{3+}	0.000	0.002	0.000	0.000	0.001	0.000	0.000	0.000	0.000	0.000
Mg	0.002	0.000	0.002	0.001	0.004	0.001	0.002	0.002	0.005	0.004
Na	0.002	0.002	0.007	0.003	0.000	0.002	0.001	0.004	0.003	0.004
K	0.001	0.002	0.003	0.000	0.001	0.001	0.000	0.002	0.000	0.001

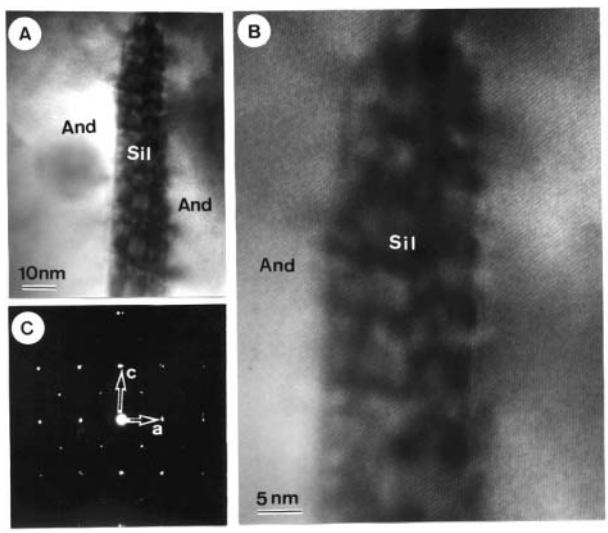

FIGURE 13. (a) Low magnification TEM image of a sillimanite lamella included in andalusite. **(b)** Higher magnification of Figure 13a showing the crystallographic continuity across the interface between the sillimanite lamella and the andalusite host. **(c)** Selected-area electron diffraction (SAED) pattern at the interface showing the slight misorientation between the two lattices equivalent to a rotation of the sillimanite lattice by approximately 2–3° around $[010]_{And}$. The labels are for the andalusite matrix.

The resulting microstructures are (001) lamellae of mullite in andalusite. The reaction front is not planar but decomposed into $\{011\}_{And}/\{201\}_{Mul}$ facets. A slight misorientation of both *c* axes by an angle of 5° around $a_{And} \parallel b_{Mul}$ can be observed. The consequence of this misorientation is that the {011} planes of andalusite are parallel to the {201} planes of mullite, e.g., precisely the facet orientation. The lattice misfit within the facets is substantially reduced compared to a $(001)_{And}/(001)_{Mul}$ interface. The misfit along $[011]_{And}/[201]_{Mul}$ is only 0.87% at room temperature compared to 4.53% along $[010]_{And}/[100]_{Mul}$, the equivalent orientation in the $(001)_{And}/(001)_{Mul}$ interface. Therefore, misfit reduction controls the boundary orientation.

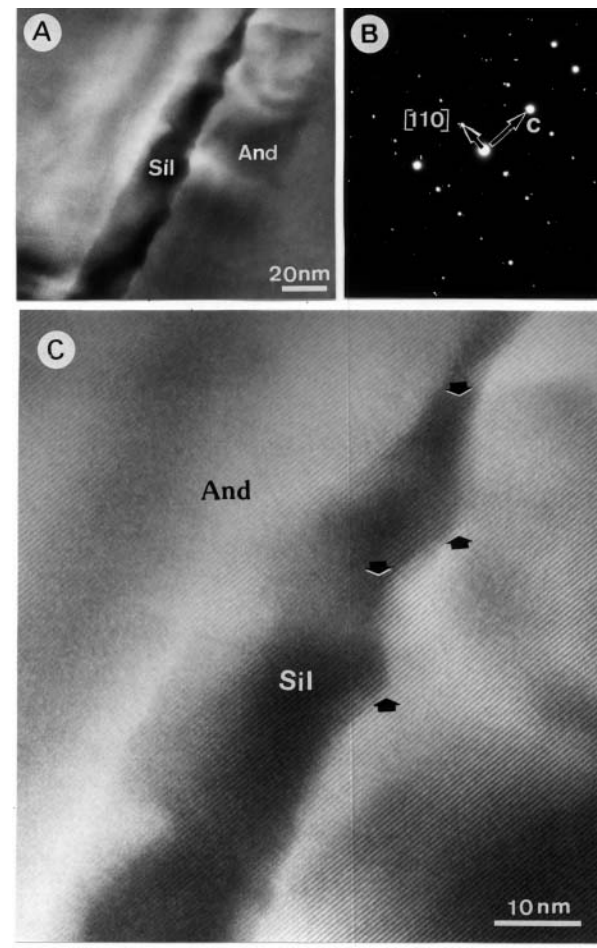

FIGURE 14. (**a**) Low-magnification TEM image of a sillimanite lamella oblique with respect to the *c* axes of sillimanite and andalusite. (**b**) Lattice fringes corresponding to the (110) planes of both phases slightly change in orientation across the boundary (Fig. 9), due to the change in orientation of their respective *c* axes. Arrows mark the traces of the $(032)_{And}/(302)_{Sil}$ interface. (**c**) Splitting of diffraction spots demonstrate change in orientation.

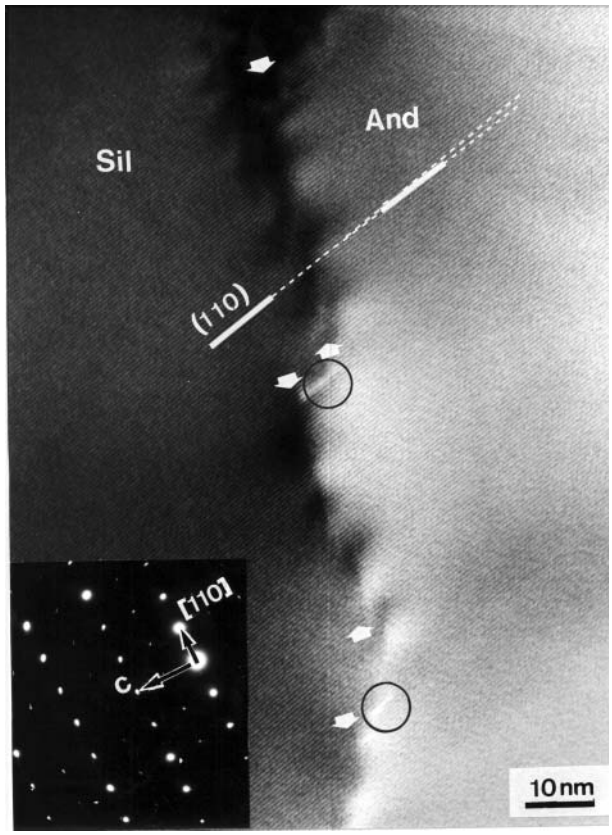

FIGURE 15. [$\bar{1}$10] HRTEM image of a stepped interface between andalusite and sillimanite at the tip of a sillimanite lamella. The (110)-lattice plane fringes with a *d*-spacing of 0.55 nm are more or less continuous, but the change in orientation of the *c* axes across the boundary (white lines) is evident. Arrows mark intervals of the interface which have an orientation lying between $(032)_{And}/(302)_{Sil}$ and $(011)_{And}/(101)_{Sil}$. Mismatch along the interface is relieved by interface dislocations (circles). Dislocations are best seen looking at a shallow angle along the *c* axis.

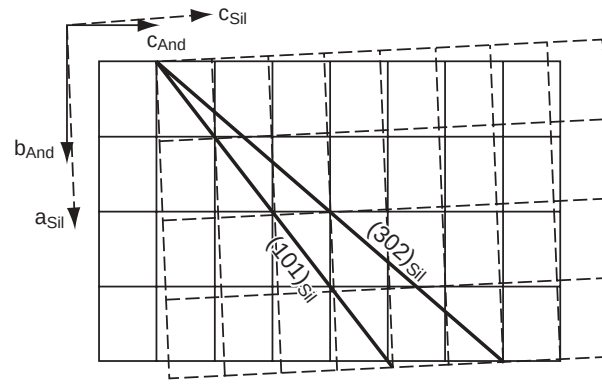

FIGURE 16. Projection of the andalusite and sillimanite lattices down the a axis of andalusite. The sillimanite lattice is rotated by 2.6° around a_{And}. The $(023)_{And}$ and $(302)_{Sil}$ are parallel and show almost no dimensional mismatch.

The misorientation angle for the andalusite-sillimanite pair is only 2–3°. A rotation by 2.52° of the sillimanite lattice around the *a* axis of andalusite causes the {011} planes of andalusite to be parallel to the {101} planes in sillimanite, a situation equivalent to the andalusite/mullite relationship described above ($c_{Sil} \sim 2c_{Mul}$). The mismatch along $a_{And} \parallel b_{sill}$ is 1.4%, but the mismatch along $[011]_{And}/[101]_{Sil}$ is 2.2%, much larger than for the mullite/andalusite case. A slightly larger rotation of 2.62° causes the {032} planes of andalusite to be parallel to the {302} planes in sillimanite. In this case the misfit is only 0.35% (room temperature, Fig. 16). The angle of 53° between the traces of the second set of facets and the (110) fringes in [$\bar{1}$10] HRTEM images (Fig. 14) is compatible with this orientation. As noted above, two sets of parallel topotactic Sil_1 are observed optically, with misorientation <6°. We propose that in one set (032) of andalusite is parallel to (302) of sillimanite and in the second set ($0\bar{3}2$) of andalusite is parallel to ($\bar{3}02$) of sillimanite. The angle between the sillimanite *c* axis of the first and second set should be 5.24° for pure sillimanite at room temperature, which is close to the observed 6°. Slight deviation (e.g., ±1°) from the ideal angle between the two *c* axes can be explained with differences in unit-cell parameters of the samples, due to impurities or different transformation temperature, and the poor measurement accuracy. Deviations by up to 16° between the *c* axes (such as measured by Rosenfeld 1969) cannot be explained by the above model, and probably represent growth of sillimanite that is not controlled by crystallography.

In the andalusite-mullite transformation, mullite nucleates along (011) planes of andalusite. For the nucleation of topotactic sillimanite, Vernon (1987) argued that the presence of deformation-induced stacking faults in andalusite (Lefebvre 1982; Doukhan et al. 1985) may be relevant. The atomic structure of stacking faults resulting from the dissociation of *c* dislocations along (010) is close to the sillimanite structure and may act as nucleation cores for sillimanite. The dissociation of the unit dislocation would transform AlO_5 bipyramids of the andalusite structure into strongly distorted AlO_4 tetrahedra. However, TEM analysis of *c*-dislocations in experimentally deformed andalusite (Lefebvre 1982) under weak-beam conditions revealed no dissociations, which limits the maximum possible dissociation width to a value smaller than the resolution of the weak-beam technique (4 nm). The only dislocations found in the samples were misfit dislocations along the interfaces. Thus, the role of strain-induced dislocations suggested by Vernon (1987) may not be directly applicable to the present study, and we favor homogeneous nucleation driven by considerable overstepping of the equilibrium temperature to be responsible for the formation of sillimanite nuclei. Such a nucleation mechanism would also explain the small number of topotactic sillimanite crystals found within the andalusite. The orientation of the interfaces for small sillimanite crystals are commonly parallel to $(032)_{And}$ (indicated by arrows in Figs. 14 and 17) suggesting that they nucleate along these planes.

The development of the lamellar morphology is usually the result of slow growth normal to the coherent/semicoherent interface and fast growth normal to the incoherent edges (Putnis 1992). In such a case, one would expect $\{302\}_{Sil}$ prisms and

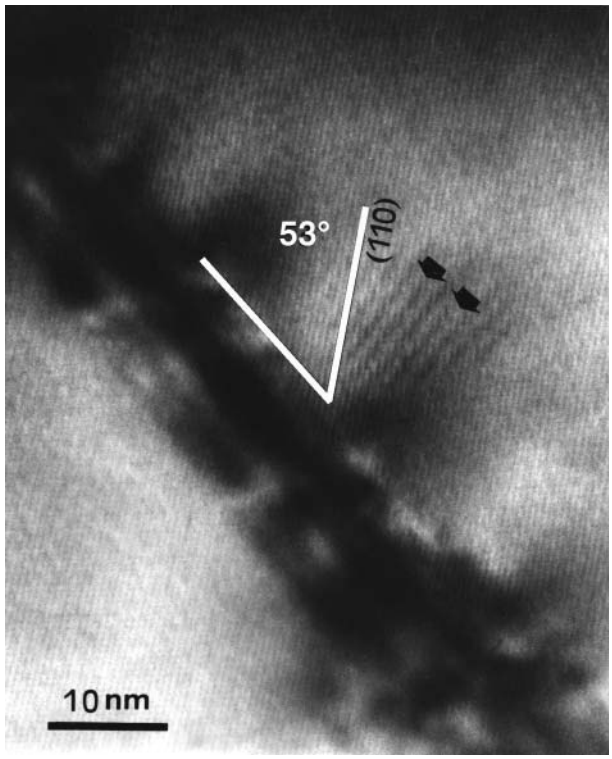

FIGURE 17. [$\bar{1}$10] HRTEM image of a small lamella of "sillimanite" within andalusite. The lattice fringes correspond to (110). The calculated angle between the trace of a $(032)_{And}$ || $(302)_{Sil}$ and the *c* axis of andalusite in such an image is 53.1° (room temperature) very close to the indicated measured value. The Moiré fringes (black arrows) occur through interference of the inclined sillimanite (302) lamella and the andalusite matrix.

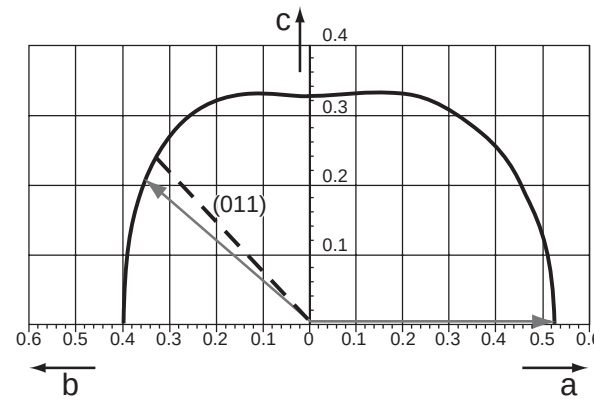

FIGURE 18. Elastic compliances (megabars^{-1}) within the (100) and (010) plane of andalusite. Grey arrows indicate the soft directions in both planes. The values were calculated using the elastic constants given by Vaughan and Weidner (1979) using the expression by Nye (1985, p. 145).

not the observed $\{hk0\}_{Sil}$ prisms. Taking elastic compliances into consideration (Fig. 18), prisms within a plane close to $(011)_{And}$ would be the most favorable, but certainly not prisms elongated parallel to the *c* axis, which is the stiffest direction in andalusite. Note that the (032) plane is close to the (011) plane, and very small crystals with that orientation (Fig. 17) are not only favored by low interfacial energies but also by the elastic softness within that plane. The macroscopic shape is thus controlled neither by interface energy minimization nor by elastic constraints. As in the andalusite/mullite case, specifics of the reaction mechanism and kinetics are the parameters dictating the shape of the growing lamellae. The transformation of andalusite to sillimanite involves a change of coordination from fivefold to fourfold for half of the Al cations, and a slight reorientation of the octahedral chains. This reconstructive inversion requires the breaking and, after slight displacement of the cations, new formation of Si-O and Al-O bonds. Diffusion distances are very short, and the newly formed Al and Si tetrahedra form double chains along the *c* axis. The strong coupling of the octahedra through the shared polyhedral edge along the *c* axis is possibly the reason for the preferential growth along the *c* axis. Rearrangement of one octahedron forces the adjacent ones along the chain to adjust, propagating the reaction along the *c* axis and leading to the observed lamellar morphology.

Activation energy for such reconstructive phase transformations is high, and large overstepping of the equilibrium conditions are necessary to see considerable reaction progress to occur. Despite enclosure in lavas that were at temperatures of ~900 °C, the xenoliths display large differences in reaction progress. This heterogeneous behavior is probably related either to temperature gradients within the magma chamber, or to variable times of interaction between xenoliths and host dacite. An additional explanation is that, if the residence time of the xenoliths in the dacite was very short, the observed differences attest to heterogeneous sampling of the anatectic crystalline basement by the uprising magma.

Other mechanisms of andalusite replacement

Along with the topotactic substitution by Sil_1, the observed microstructures indicate additional mechanisms for the replacement of andalusite. Andalusite is resorbed, and embayed grain boundaries are filled by fibrolite and plagioclase, cordierite, or graphite (Figs. 3 and 4). Fibrolite is also widespread in the matrix away from andalusite. These microstructures are indicative of dissolution of andalusite and precipitation of fibrolite and other phases. Dissolution of andalusite is probably favored along (110) cleavage planes, thereby creating space for the growth of fibrolite needles (Fig. 5). There seems to be no crystallographic control by the receding cleavage planes on the orientation of the needles. This is not a real crystallographic control but rather depends on the morphology of the dissolved gap, which favors the growth of needles parallel to the cleavage plane. On the crystal surface, where pervasive dissolution gave rise to large embayments, the orientation of the fibrolite axes was not controlled anymore, leading to the formation of random to radiating aggregates of fibrolite (Fig. 4).

This dissolution-precipitation process is similar to the "ionic" reaction mechanism proposed by Carmichael (1969) for the Ky-Sil reaction. We have not tried to balance the possible reaction of andalusite dissolution, but we infer that this

reaction was probably accompanied by a C-O-H fluid and/or a silicate melt phase. The presence of a carbonic fluid, discussed in detail by Cesare and Maineri (1999) is supported by the systematic occurrence of fine-grained graphite intergrown with fibrolite.

The convex andalusite boundaries and the associated fibrolite crystals (Fig. 4) seem to have originated in the same way as the convex interfaces between andalusite and silica glass observed by Hülsmans et al. (2000b). They interpreted those interfaces as a result of a melt-assisted dissolution/precipitation process. The mechanism of dissolution-precipitation, assisted by fluid or melt, is the main process for the development of fibrolite in these xenoliths. Because fibrolite is not in direct contact with andalusite, this process shows similarities to many observations from low-pressure contact aureoles (e.g., Vernon 1987).

We have shown that andalusite is also locally replaced by prismatic Sil_2, which may form by coalescence and/or coarsening of earlier fibrolite (see below) related to the above dissolution-precipitation process. In this case, graphite or other phases are commonly preserved at the And-Sil_2 interface. In rare occasions, such Sil_2 prisms cross into andalusite crystals (Fig. 10).

DISCUSSION

A geological model for the replacement of andalusite by sillimanite

The xenoliths contain various generations of Al_2SiO_5 polymorphs, and were involved in a complex geologic history including regional metamorphism, anatexis, and incorporation in the dacitic magma. Because andalusite and/or sillimanite may have grown during each of these stages, it is important to constrain their origin in the temporal sequence of events that occurred to the metapelitic protoliths as they were converted into the xenoliths. The primary obstacle to this reconstruction is that there is no direct access to the source of the xenoliths, i.e., to the crystalline basement underlying the Neogene Volcanic Province. Thus, data from neighboring areas are used as the best constraints of the starting configuration of the studied samples. In addition, there is no guarantee that all the xenoliths shared an unique history, so that they may provide contrasting indications, which may not, and probably need not, agree with each other.

The crystalline basement of the Betic-Alborán domain is composed of mostly graphitic metasediments, in which coexisting andalusite and fibrolite are widely reported (e.g., Soto and Platt 1999), but where the association of andalusite and oriented sillimanite has not been observed. Although partial melting is believed to have occurred (Soto and Platt 1999), there is no evidence of primary melt inclusions (either fresh or recrystallized) in the minerals of these metapelites, and in particular in andalusite. The high-grade metamorphism in the crystalline basement of the Betic-Alborán domain is dated at 27–20 Ma (Comas et al. 1999; Platt and Whitehouse 1999). Owing to their petrographic features, the And-Sil-bearing paragneisses and migmatites of this basement may constitute the source rocks for the xenoliths, but lower-grade metapelites may equally represent appropriate protoliths.

With respect to the partial melting event, the peculiar microstructures developed in the xenoliths indicate that (1) partial melting was (or commenced as) syntectonic, i.e., prior to incorporation in the magma and (2) growth of andalusite with melt inclusions (or part of it) also took place before incorporation in the dacite. Zircon SHRIMP data (D. Rubatto, personal communication) indicate that at Mazarrón partial melting and lava eruption were almost coeval at 9.6 Ma.

The last microstructural event, as revealed by the And-Sil replacement, is probably the least constrained. It may have occurred both before and after enclosure of the xenoliths and xenocrysts in the dacite. Microstructures such as the slight bending of sillimanite prisms would suggest the first possibility, but in other cases sillimanite growth seems to be post-tectonic, which might suggest the second option. Thus, both interpretations are plausible, and we cannot exclude that both are valid, if the xenoliths do not provide evidence for a unique geologic history. An additional possibility is that the And-Sil replacement was prolonged in time, starting before, and continuing after entrapment of the rock fragments in the dacitic magma.

Andalusite metastability at high temperatures

Andalusite is commonly preserved in the xenoliths and xenocrysts of the lavas of Mazarrón, even in the samples where sillimanite is abundant. Thus, despite the microstructural evidence of replacement by sillimanite, andalusite relicts persist deep into the the stability field of sillimanite. Chemical data (Table 1) preclude the possibility that stability relationships between the two polymorphs have been affected by partitioning of minor elements.

Andalusite metastability is widely inferred in contact aureoles (e.g., Pattison 1992, and references therein), and its cause is attributed to the small ΔS of the And-Sil polymorphic inversion. Field observations show that andalusite and sillimanite may co-exist over an area corresponding to a large temperature interval and that a large overstepping of the And-Sil equilibrium is required for the complete disappearance of andalusite (e.g., Wickham 1987; Kerrick and Woodsworth 1989). The present study is of particular importance because of the very high temperatures (800–900 °C) attained by the xenoliths. If we consider equilibration pressures in the range 3–4 kbar, we can deduce minimum overstepping values of ~250 °C or ~150 °C, assuming the triple points of Holdaway (1971) or Pattison (1992), respectively. This example confirms the observations of Speer (1982) that andalusite also persists metastably in granulite-facies assemblages. The possible causes for the metastability of andalusite at such high temperatures may be the short duration of the anatectic event and short time of residence of xenoliths in the magma.

In some natural examples of rapidly heated xenoliths (e.g., Wehr volcano, Germany, Grapes 1986; Ross of Mull, Scotland, Brearley 1987) and in kinetic experimental simulations of contact metamorphism (e.g., Brearley and Rubie 1990), metastable behavior is commonly indicated by the product phases of melting reactions (e.g., metastable melts and mullite). Conversely, in the xenoliths of Mazarrón there is no evidence of metastable products, and metastability is essentially recorded by the persistence of andalusite far beyond its thermal stability limit.

The reported evidence that andalusite crystallized in the presence of a silicate melt may indicate either andalusite-melt

equilibrium, or metastable andalusite growth in the sillimanite stability field. The first possibility would be of particular petrogenetic interest, as discussed by Pattison (1992), but is difficult to prove. The equal, low Fe contents of andalusite and sillimanite indicate that the And-Sil equilibrium was not displaced; however, in the absence of data on the F and B contents of the glass inclusions, we cannot estimate the possible depression of the partial melting curve toward lower temperatures.

Coarsening/coalescence of fibrolite to sillimanite

In the observed microstructures, fibrolite commonly coexists with both types of prismatic sillimanite (Sil_1 and Sil_2). The existence of myriads of fibers within microscopic domains indicates that low activation energy must be assumed for the nucleation of fibrolite (e.g., Kerrick 1990). Conversely, the transition from fibrolite to coarser prisms seems to be slow. In our case (Fig. 6), this transition is observed frequently in the case of Sil_2, and very rarely for Sil_1. Coarsening occurs both by the Ostwald ripening mechanism, where the smallest fibers dissolve and reprecipitate onto larger crystallites, or by coalescence of favorably oriented, subparallel needles of fibrolite. Vernon (1987) has described similar microstructures in contact-metamorphosed metapelites, but the coarsening of fibrolite to sillimanite is not a common process in metamorphic rocks. The difficulty of recrystallizing fibrolite needles with diameters >1 μm has been justified by Wintsch (personal communication in Kerrick 1990) on the basis of their low-grain boundary energy. Alternative causes for the refractory behavior of fibrolite may be difficulties in the transport of matter, namely the low solubility of Al_2O_3 in hydrous or silicate fluids (Hülsmanns et al. 2000b), or the slow rate of dissolution-precipitation processes at fibrolite crystal surfaces. This last possibility agrees with the slow precipitation-dissolution rates at andalusite surfaces observed experimentally by Schramke et al. (1987) and Hülsmanns et al. (2000b).

Along with the metastable persistence of andalusite in the sillimanite field, the present work confirms the sluggish kinetics of the coarsening of fibrolite. These phenomena, commonly reported from contact aureoles, have been here observed in a high-temperature (granulite-facies) setting. The kinetic difficulties of the coarsening process are even more evident in the xenoliths of other volcanic edifices of the Neogene Volcanic Province of SE Spain. In particular, the xenoliths at El Joyazo (Cesare et al. 1997; Cesare and Gómez-Pugnaire 2001) contain only fibrolite as the Al_2SiO_5 polymorph, and have been partially melted at temperatures up to 900 °C (Cesare 2000). Although zircon SHRIMP data (D. Rubatto, personal communication) suggest that at El Joyazo the high-temperature conditions lasted at least 2.5 m.y., no evidence of fibrolite coarsening is observed in these rocks.

The microscopic lamellae of "sillimanite" observed in this TEM study should be, according to the size definition, addressed as fibrolite. These lamellae are obviously not visible by optical microscopy. The distribution of the size populations of optically visible sillimanite crystals has a clear lower cut-off that is above the resolution of the microscope. We suggest that many reported occurences of unreacted andalusite coexisting with fibrolite may reveal, if looked at with the right "glasses" (e.g., by TEM), situations where andalusite has already commenced its topotactic inversion to sillimanite.

ACKNOWLEDGMENTS

Financial support from Università di Padova, Fondi Progetti Ricerca 1998 (to B.C.), DGICYT Project BTE 2000-0582 (to A.S.N.), and RNM-0145 Group of Research of the Junta de Andalucía (to M.T. G.P.). We thank A. Brearley, D.M. Carmichael, and B. Dutrow for their helpful reviews, M.M. Abad (Centro de Instrumentación Científica de la Universidad de Granada) for help with the TEM, and B. Provincias for fruitful discussions.

REFERENCES CITED

Bellon, H., Bordet, P., and Montenat, C. (1983) Chronologie du magmatisme Nèogéne des Cordilléres Bètiques (Espagne Mèridionale). Bulletin Société Géologique de France, 25, 205–217.

Benito, R., Lopez-Ruiz, J., Cebriá, J.M., Hertogen, J., Doblas, M., Oyarzun, R., and Demaiffe, D. (1999) Sr and O isotope constraints on source and crustal contamination in the high-K calc-alkaline and shoshonitic Neogene volcanic rocks of SE Spain. Lithos, 46, 773–802.

Brearley, A.J. (1987) A natural example of the disequilibrium breakdown of biotite at high temperature; TEM observations and comparison with experimental kinetic data. Mineralogical Magazine, 51, 93–106.

Brearley, A.J. and Rubie, D.C. (1990) Effects of H_2O on the disequilibrium breakdown of muscovite+quartz. Journal of Petrology, 31, 925–956.

Carmichael, D.M. (1969) On the mechanism of prograde metamorphic reactions in quartz-bearing pelitic rocks. Contributions to Mineralogy and Petrology, 20, 244–267.

Cesare, B. (2000) Incongruent melting of biotite to spinel in a quartz-free restite at El Joyazo (SE Spain): Textures and reaction characterization. Contributions to Mineralogy and Petrology, 139, 273–284.

Cesare, B. and Gómez-Pugnaire, M.T. (2001) Crustal melting in the Alborán domain: constraints from the xenoliths of the Neogene Volcanic Province. Physics and Chemistry of the Earth, A, 26, 255–260.

Cesare, B. and Maineri, C. (1999) Fluid-present anatexis of metapelites at El Joyazo (SE Spain): constraints from raman spectroscopy of graphite. Contributions to Mineralogy and Petrology, 135, 41–52.

Cesare, B., Salvioli Mariani, E., and Venturelli, G. (1997) Crustal anatexis and melt extraction in the restitic xenoliths at El Joyazo (SE Spain). Mineralogical Magazine, 61, 15–27.

Comas, M.C., Platt, J.P., Soto, J.I., and Watts, A.B. (1999) The origin and tectonic history of the Alborán Basin: Insights from Leg 161. In R. Zahn, M.C. Comas, and A. Klaus, Eds., Proceedings of the Ocean Drilling Program, Scientific Results, 161, 555–579. Ocean Drilling Program, College Station, TX.

Doukhan, J.C., Doukhan, N., Koch, P.S., and Christie, J.M. (1985) Transmission electron microscopy investigation of lattice defects in Al_2SiO_5 polymorphs and plasticity induced polymorphic transformations. Bulletin de Minéralogie, 108, 81–96.

Glen, R.A. (1979) Evidence for cyclic reactions between andalusite, "sericite" and sillimanite, Mount Franks area, Willyama Complex, N.S.W. Tectonophysics, 58, 97–112.

Grapes, R.H. (1986) Melting and thermal reconstitution of pelitic xenoliths, Wehr volcano, East Eifel, West Germany. Journal of Petrology 27, 343–396.

Harker, A. (1939) Metamorphism. 362 p. Chapman and Hall, London.

Holdaway, M.J. (1971) Stability of andalusite and the aluminum silicate phase diagram. American Journal of Science, 271, 97–131.

Hülsmans, A., Schmücker, M., Mader, W., and Schneider, H. (2000a) The transformation of andalusite to mullite and silica: Part I. Transformation mechanism in $[001]_A$ direction. American Mineralogist, 85, 980–986.

———(2000b) The tranformation of andalusite to mullite and silica: Part II. Tranformation mechanisms in $[100]_A$ and $[010]_A$ directions. American Mineralogist, 85, 987–992.

Kerrick, D.M. (1990) The Al_2SiO_5 polymorphs, vol. 22, 406 p. Reviews in mineralogy, Mineralogical Society of America, Washington, D.C.

Kerrick, D.M. and Speer, J.A. (1988) The role of minor element solid solution on the andalusite-sillimanite equilibrium in metapelites and peraluminous granitoids. American Journal Science, 288, 152–192.

Kerrick, D.M. and Woodsworth, G.J. (1989) Aluminum silicates in the Mount Raleigh pendant, British Columbia. Journal of Metamorphic Geology, 7, 547–563.

Kretz, R. (1983) Symbols for rock-forming minerals. American Mineralogist, 68, 277–279.

Lefebvre, A. (1982) Transmission electron microscopy of andalusite single crystals indented at room temperature. Bulletin de Minéralogie, 105, 347–350.

Molin, D. (1980) Le volcanisme miocene du Sud-Est de l'Espagne Provinces de Murcia et d'Almeria. PhD Thesis, Univ. Paris VI, 289 p.

Nye, J.F. (1985) Physical properties of crystals. Oxford University Press, Oxford.

Papike, J.J. (1987) Chemistry of the rock-forming silicates: ortho, ring, and single-

chain structures. Reviews in Geophysics, 25, 1483–1526.
Pattison, D.R.M. (1992) Stability of andalusite and sillimanite and the Al_2SiO_5 triple point: Contraints from the Ballachulish aureole, Scotland. Journal of Geology, 100, 423–446.
Pichavant, M., Kontak, D.J., Valencia Herrera, J., and Clarck, A.H. (1988) The Miocene-Pliocene Macusani volcanics, SE Peru 1. Mineralogy and magmatic evolution of a two-mica aluminosilicate-bearing igninbrite suite. Contributions to Mineralogy and Petrology, 100, 300–324.
Platt, J.P. and Whitehouse, M.J. (1999) Early Miocene high-temperature metamorphism and rapid exhumation in the Betic Cordillera (Spain): evidence from U–Pb zircon ages. Earth and Planetary Science Letters, 171, 591–605.
Putnis, A. (1992) Introduction to Mineral Sciences, 457 p. Cambridge University Press, New York.
Rosenfeld, J.L. (1969) Stress effects around quartz inclusions in almandine and the piezothermometry of coexisting aluminium silicates. American Journal Science, 267, 317–351.
Schramke, J.A., Kerrick, D.M., and Lasaga, A.C. (1987) The reaction muscovite + quartz = andalusite + K-feldspar + water. Part I. Growth kinetics and mechanism. American Journal of Science, 287, 517–559.
Soto, J.I. and Platt, J.P. (1999) Petrological and structural evolution of high-grade metamorphic rocks from the floor of the Alborán Sea basin, western Mediterranean. Journal of Petrology, 40, 21–60.
Speer, J.A. (1982) Metamorphism of the pelitic rocks of the Snyder Group in the contact aureole of the Kiglapait layered intrusion, Labrador: effects of buffering partial pressures of water. Canadian Journal of Earth Sciences, 19, 1888–1909.
Turner, S.P., Platt, J.P., George, R.M.M., Kelley, S.P., Pearson, D.G., and Nowell, G.M. (1999) Magmatism associated with orogenic collapse of the Betic-Alborán Domain, SE Spain. Journal of Petrology, 40, 1011–1036.
Vaughan, M.T. and Weidner, D.J. (1979) The relationship of elasticity and crystal structure in andalusite and sillimanite. Physics and Chemistry of Minerals, 3, 133–144.
Vernon, R.H. (1987) Oriented growth of sillimanite in andalusite, Placitas-Juan Tabo area, New Mexico, U.S.A. Canadian Journal of Earth Sciences, 24, 580–590.
Walther, J.V. and Wood, B.J. (1984) Rate and mechanism in prograde metamorphism. Contributions to Mineralogy and Petrology, 88, 246–259.
Wickham, S.M. (1987) Crustal anatexis and granite petrogenesis during low-pressure regional metamorphism: the Trois Seigneurs Massif, Pyrenees, France. Journal of Petrology, 28, 127–169.
Winter, J.K. and Ghose, S. (1979) Thermal expansion and high-temperature crystal chemistry of the Al_2SiO_5 polymorphs. American Mineralogist, 64, 573–586.
Zeck, H.P. (1970) An erupted migmatite from Cerro de Hoyazo, SE Spain. Contributions to Mineralogy and Petrology, 26, 225–246.

MANUSCRIPT RECEIVED MAY 8, 2001
MANUSCRIPT ACCEPTED DECEMBER 1, 2001
MANUSCRIPT HANDLED BY BARB DUTROW